2015 IEEE/SICE International Symposium on System Integration (SII)
December 11-13, 2015. Meijo University, Nagoya, Japan

System Integration of a Solar Sensor and a Spherical Parallel Manipulator for a 3-Axis Solar Tracker Platform Design

Bukeikhan Omarali, Tasbolat Taunyazov, Aibek Nyetkaliyev and Almas Shintemirov

Abstract— **This paper presents the authors' ongoing work on designing a novel 3-axis solar tracker platform utilizing a 3-DOF spherical parallel manipulator with revolute joints and a solar sensor. The selected solar sensor and the SPM configuration are described in details. A novel approach is proposed for the SPM platform orientation estimation based on solar sensor measurements employing trigonometric identities and quaternion rotation representation. The proposed approach is experimentally verified using a SPM 3D-printed prototype equipped with a solar and an orientation sensors. It is assumed that the proposed concept for a novel 3-axis solar tracker platform can further applied to design novel mobile solar tracking systems.**

I. INTRODUCTION

At the moment, there are mainly two types of solar trackers are in common use: single-axis and dual-axis solar trackers. Single-axis solar trackers have one degree-of-freedom (DOF), that is an axis of rotation, as shown in Fig. 1(a). This axis of rotation is usually oriented along the North meridian. More advanced dual-axis solar trackers are characterized by two axes of rotation are 2-DOF systems (Fig. 1(b)). These axes are generally perpendicular to each other. The dual-axis trackers optimize the use of solar energy due to their ability to follow the Sun vertically and horizontally. They can be positioned to be in the constant direct contact with the Sun.

In general, dual-axis solar trackers constitute a serial configuration and, as in all series kinematics systems, the tracking error represents the sum of the two actuators errors. Normally, this leads to the use of the costly high precision reduction boxes for reducing the cumulative tracking error and maximization of energy generation.

To overcome these drawbacks of traditional 2-axis solar tracker platforms, parallel manipulators can be considered as an alternative. Comparing to series kinematic designs, parallel manipulators provide higher stiffness and load-carrying capacity and excellent dynamic properties since the inertia of the moving parts of a parallel manipulator is considerably reduced. This is achieved due to the connection of the top mobile platform of a manipulator via multiple kinematic chains to the manipulator base and the fact that the actuators can be located on or close to the base [1]. Thus, alternative 3-DOF parallel manipulator based solar tracker platforms will be able to carry geometrically larger and more massive photovoltaic modules, while employing less powerful system actuators and gearboxes. this leads to similar or even lower total cost of such solar systems comparing to the traditional dual-axis trackers despite the use of an additional actuator in the novel 3-DOF solar tracker designs. In addition, the overall tracking error of the 3-DOF solar tracking systems will be determined by the largest error of one of the systems actuators.

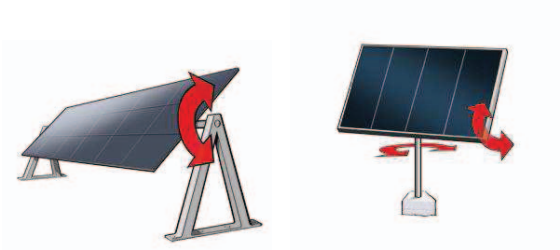

(a) (b)

Fig. 1. A single-axis solar tracker (a), and a dual-axis solar tracker configurations (b).

Among numerous types of parallel manipulators, spherical parallel manipulators (SPMs) can be applied for designing 3-DOF systems capable of operating over a large hemisphere workspace and high dynamics. A special case of a 3-DOF SPM with revolute joints (RRR type) named Agile Eye is proposed in [2] for designing a novel camera orientation system. A modification of the Agile Eye, the Agile Wrist, with enhanced load-carrying capacity and reduced weight, is extensively studied in [3], [4].

In this paper, the authors present preliminary results on designing a 3-axis solar tracker platform utilizing a 3-DOF SPM with revolute joints and a solar sensor. A novel approach for the SPM platform orientation estimation is proposed based on the solar sensor measurements employing trigonometric identities and quaternion rotation representation. Experimental verification of the proposed approach is presented using an SPM 3D printed prototype equipped with a solar and an orientation sensors. The system is designed with mobile applications in mind more of which is discussed in the future work section at the end.

This work was supported by the Kazakhstan Ministry of Science and Education through the program-target funding scheme as part of the "Research of Possible Applications of Renewable Energy for Development of Small/Mobile Autonomous Systems" project within the "Research and Development in the Field of Energy Efficiency and Conservation, Renewable Energy and Environmental Protection in 2014-2016" research program.

B. Omarali is with the Department of Mechanical Engineering, School of Engineering, and Nazarbayev University Research and Innovation System, Nazarbayev University, Astana, Kazakhstan.

T. Taunyazov, A. Nyetkaliyev and A. Shintemirov are with the Department of Robotics and Mechatronics, School of Science and Technology, and National Laboratory Astana, Nazarbayev University, Astana, Kazakhstan.

Corresponding author: A. Shintemirov, ashintemirov@nu.edu.kz

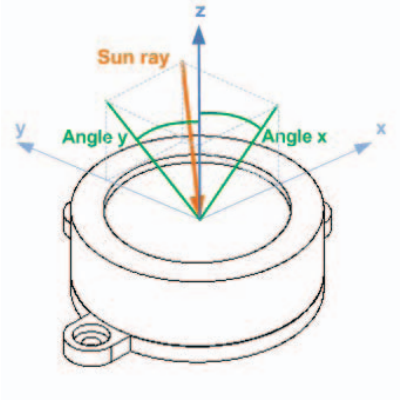

Fig. 2. MASS60 solar sensor [8].

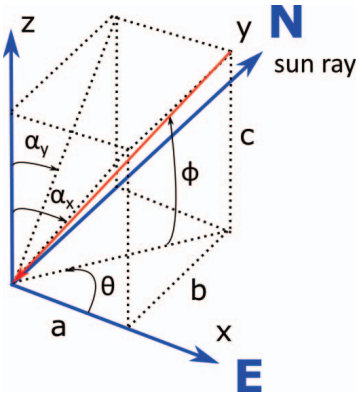

Fig. 3. MASS60 solar sensor coordinate system, output angles and processed azimuth and elevation angles.

II. SOLAR SENSOR

Solar tracker systems largely use solar sensors to determine the position of the Sun and orient the solar panels accordingly for maximum power generation. It is expected that the solar tracker platform motion will put the Sun at large angle to the PV panels. Therefore, it is preferable to select a solar sensor with a large field of view. However, it is known that there is a general trade-off between the field of view and accuracy characteristics of the sensors, especially for terrestrial applications where reflected and scattered light imposes considerable errors on light sensitive elements in sensors.

In general solar sensors can be divided into analog and digital solar sensors. Analog solar sensors use a set of photodiodes that are arranged in a certain geometry such that ratios of currents generated by photodiodes can be used to determine the relative position of the sun. Digital solar sensor use pinhole cameras and an active pixel sensor detection plane such that sun position is determined by centroiding the projective image. Such sensors are described in e.g. [5]–[7].

Comparative analysis of various commercially available solar sensors has led the authors to the selection of the digital MASS60 sensor from Solar-MEMS [8] (Fig. 5) as a sensor of choice for the preliminary 3-DOF SPM based solar tracker design. The MASS60 sensor is a lightweight, small sized and highly accurate device with a reduced cost. The sensor works as follows: incident angles of the Sun rays enter to the small window of the sensor, and it is orientation is determined by α_x and α_y angles as shown in Fig. 2. Here, α_x is an angle that the z-axis makes with the Sun ray projection onto the xz plane. Similarly, the α_y is an angle between the z-axis and the Sun ray projection onto the yz plane. These output angles are then used to determine the Sun position within the local coordinate system of the sensor in the form of the elevation ϕ and azimuth θ angles, that are subsequently used to calculate reference signals for the orientation control of the solar tracker platform.

The angles α_x and α_y can be defined by sides of the cube in Fig. 3 using trigonometric identities as follows:

$$\tan\alpha_x = \frac{a}{c} \text{ and } \tan\alpha_y = \frac{b}{c}, \tag{1}$$

that leads to the following equality

$$\frac{\tan\alpha_y}{\tan\alpha_x} = \frac{b}{a}. \tag{2}$$

The azimuth angle θ is measured around the z-axis from the x-axis in the north-west direction. On the xy plane θ is calculated as follows

$$\tan\theta = \frac{a}{b}. \tag{3}$$

Combining equations (2) and (3) results to

$$\theta = \arctan\left(\frac{\tan\alpha_y}{\tan\alpha_x}\right). \tag{4}$$

Since the azimuth is the rotation around the z-axis, equation (4) has solutions in four quadrants on the xy plane. Furthermore, when the x-axis is aligned with the Earth's north magnetic vector the azimuth angle is counted northwestwardly. Since the general convention is to estimate the azimuth angle in the north-eastward direction, the given azimuth should be transformed when comparing to the Sun ephemeris results θ (equation (5)).

$$\theta_{NE} = 2\pi - \theta \tag{5}$$

Analogously, the same trigonometry method applied to find the elevation angle ϕ as follows:

$$\phi = \arctan((\tan^2\alpha_x + \tan^2\alpha_y)^{-\frac{1}{2}}). \tag{6}$$

III. SPHERICAL PARALLEL MANIPULATOR

A model of a general symmetric 3-DOF SPM with revolute joints is shown in Fig. 4. The SPM consists of two pyramid-shape platforms: a base and a top mobile platform. These are connected by three equally-spaced legs, numbered by $i = 1, 2, 3$, each of them composed of two curved links, namely proximal (lower) and distal (upper) links. The axes of all joints, denoted by unit vectors $\mathbf{u}_i$, $\mathbf{v}_i$, and $\mathbf{w}_i$, intersect at a common center of rotation point. The dimensions of proximal and distal links are denoted as α_1

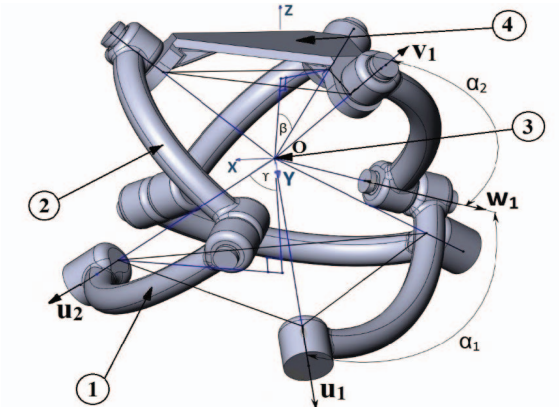

Fig. 4. 3D representation of the kinematic model of a 3-DOF RRR SPM: (1) - proximal link, (2) - distal link, (3) - center of rotation, (4) - top mobile platform.

Fig. 5. The experimental setup, consisting of a 3D printed prototype of the Agile Wrist SPM, a MASS60 solar sensor and a Oriel Sol3A solar simulator.

and α_2, respectively. Angles β and γ define the geometry of two regular pyramids of the top mobile and base platforms. The motion of the top mobile platform is confined on the surface of a sphere centered at the center of rotation.

The right-handed orthogonal coordinate system with its origin located at the SPM center of rotation is shown in Fig. 4. The z axis is normal to the base pyramid platform and is directed upwards, while the y axis is located in the plane generated by the z axis and $\mathbf{u}_1$. The input joint angles, which can be imposed by using three electrical servomotors, are referred to as θ_i, $i = 1, 2, 3$, and measured from the plane generated by the z axis and $\mathbf{u}_i$, to the plane of a proximal link [9].

The SPM kinematics was extensively analyzed in e.g. [4], [10], [11]. In [10] it is shown that the forward kinematic problem of a general 3-DOF RRR SPM leads to a polynomial with at most eight solutions, corresponding to different poses of the manipulator top mobile platform, for a given set of control inputs. However, only one, i.e., unique, kinematic solution, corresponding to the actual physical pose of a parallel manipulator, needs to be defined for developing the SPM orientation control system. To address this problem and provide a basis for the design of a real-time SPM orientation control system, the authors developed an original framework for generating optimal motor trajectories for a SPM with revolute joints, actuated by servomotors with default internal position control settings [12]. The proposed framework consists of three phases. First, unique forward and inverse kinematic solutions are obtained, in order to relate the angular positions of the servomotors to the orientation of the SPM top mobile platform. Then, a configuration space for the SPM is defined by using numerical procedures, in order to guarantee the absence of singularities and collisions between links during the manipulator motion. Finally, reference trajectories of the servomotors are generated via convex optimization. These trajectories determine an optimal evolution of the SPM motion, based on configuration space and original servomotor dynamics.

The SPM orientation can be defined using quaternion-based mathematical description of vector rotation in Cartesian space. In fact, the quaternion representation allows to avoid the "gimbal lock" problem appearing when using traditional Euler angles [13]. To move the SPM top mobile platform only vector $\mathbf{v}_i$, $i = 1, 2, 3$ are sufficient to be mapped to the rotated coordinate system. These vectors are parallel to the axes of SPM top revolute joints as shown in Fig. 4. Rotations are performed by inverse quaternion multiplications with vectors as follows [13]:

$$\mathbf{v}_{ii} = \mathbf{q}^*_{inv}\, \mathbf{v}_i\, \mathbf{q}_{inv} \quad \text{where} \quad \mathbf{q}_{inv} = \frac{\mathbf{q}^*}{\|q\|}. \tag{7}$$

Here, $\mathbf{v}_{ii}$, $ii = 1, 2, 3$ are the new vectors rotated in the local coordinate system. These vectors define the goal position of SPM top mobile platform. $\mathbf{q}^*$ is a quaternion conjugate [13].

For Sun tracking, the azimuth θ and elevation ϕ angles, obtained from equations (4) and (6) respectively, constitute a quaternion $\mathbf{q}$ that represents the rotation of the z unit vector to the Sun ray position. This quaternion combines the sequence of rotations: first around the y-axis by the angle $\pi/2 - \phi$ (8) and then around the z-axis by the angle θ (9).

$$\mathbf{q}_1 = \begin{bmatrix} \cos\left(\frac{\frac{\pi}{2}-\phi}{2}\right) & 0 & \sin\left(\frac{\frac{\pi}{2}-\phi}{2}\right) & 0 \end{bmatrix}^\mathsf{T}. \tag{8}$$

$$\mathbf{q}_2 = \begin{bmatrix} \cos\left(\frac{\theta}{2}\right) & 0 & 0 & \sin\left(\frac{\theta}{2}\right) \end{bmatrix}^\mathsf{T}. \tag{9}$$

$$\mathbf{q} = \mathbf{q}_2 \otimes \mathbf{q}_1. \tag{10}$$

Note that $\otimes$ represents quaternion multiplication and $\mathbf{q}_2$ comes before $\mathbf{q}_1$ since the resulting quaternion q will be used for point rotation.

IV. SOLAR TRACKER PLATFORM DESIGN

A. Laboratory Setup

The laboratory setup of the 3-DOF solar tracker consists of the Agile Wrist prototype and a MASS60 solar sensor as shown in Fig. 5. In this work, the authors utilize the proposed framework for integrating a SPM platform with a solar sensor aiming to undertake the proof-of-concept experimental studies on the 3-DOF solar tracker design. For this purpose,

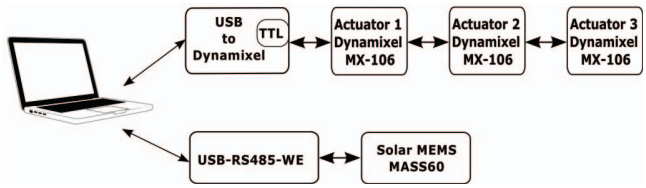

Fig. 6. Communication diagram of the 3-axis solar tracker laboratory setup.

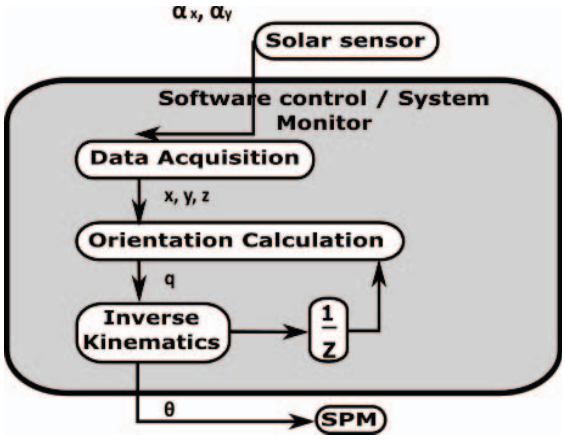

Fig. 7. Control system structure of the 3-axis solar tracker.

Fig. 8. Control task timing of the 3-axis solar tracking system.

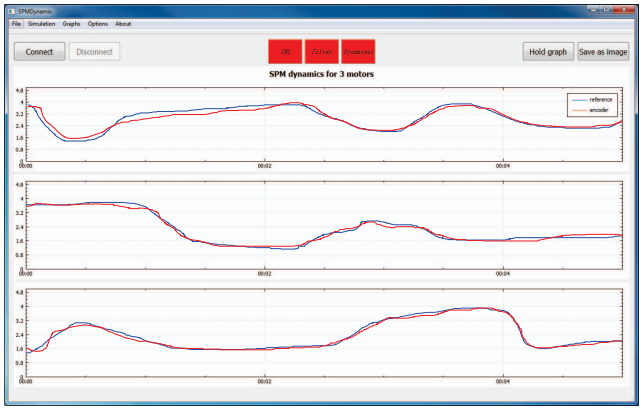

Fig. 9. The 3-axis solar tracker GUI monitoring the platform dynamics.

a small scale prototype of the "Agile Wrist" SPM has been manufactured as shown in Fig. 5. The mechanical part of the prototype has been designed in SolidWorks CAD software and manufactured using 3D printing technology with ABS plastic. The SPM prototype is actuated by three Dynamixel MX-106 servomotors fixed to the SPM base platform and controlled by a CM-700 Dynamixel servo controller. In the Agile Wrist SPM configuration $\alpha_1 = \alpha_2 = 90°$, with all three legs being identical. The three unit vectors $\mathbf{u}_i$ as well as $\mathbf{v}_i$, $i = 1, 2, 3$, are mutually orthogonal [4]. This leads to angles $\beta = \gamma = 54.7°$.

The Agile Wrist prototype and the MASS60 solar sensor are controlled from a control PC workstation. The data transmission between the SPM actuators and the PC are accomplished through TTL serial communications with 115200 baud rate using a serial-to-USB converter (USB-2-Dynamixel). The solar sensor is interfaced to the control PC via a USB-to-RS485 converter. Figure 6 demonstrates the communication diagram of the 3-axis solar tracker platform laboratory setup.

B. Control System Design

Since the Sun position changes slowly, the solar tracking process does not impose fast control response time. Thus, the solar tracker control can be realized as a soft real-time system with multiple concurrent processes (tasks) shown in Fig. 7. In general, solar trackers can be considered as non-critical systems. An event of a late deadline occurrence in one of the system control tasks would likely to cause only a short-time degradation of the power generation efficiency, while an overall behavior of the solar system will be kept unchanged.

The control algorithms are implemented as a graphical user interface (GUI) toolkit written in C++ Qt cross-compilation programming environment [14]. Qt is very useful for developing multi-threaded GUI applications efficiently utilizing multi-core processor capabilities of a control PC. The detailed timing of the control system tasks is presented in Fig. 8.

The developed control software for the solar tracker laboratory setup consists of 4 threads communicating with each other. Each thread strictly handles a separate task defined as follows.

- **GUI main** *thread*. The thread communicates with the user, monitor other child threads and interrupts. It also creates and starts all threads and reports detected errors. The GUI, implemented in this thread, visualizes the 3D orientation of the top mobile platform of a solar tracker platform using OpenGL library tools. Figure 9 demonstrates the real-time track of motion for the three SPM actuators visualized in the Qt GUI. It is shown that the actual actuator motions follow the imposed reference trajectories.
- **Data Acquisition** *thread*. This thread communicates with the solar sensor, parses and filters the sensor measurements.
- **Orientation Calculation** *thread*. The main task of this thread is to convert the input measurement data obtained from the solar sensor in the Data Acquisition thread to the reference SPM orientation values.
- **SPM Control Framework** *thread*. This thread implements the SPM control algorithms, i.e. calculates SPM inverse kinematics and trajectory generation using the reference orientation data with the purpose to obtain

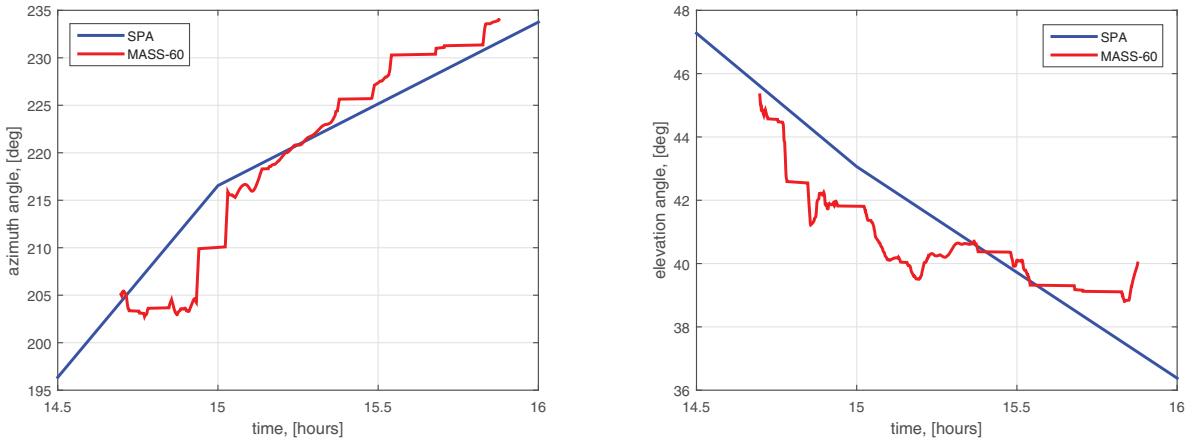

(a) (b)

Fig. 10. Verification of the azimuth (a) and elevation (b) angles with SPA.

sequence of corresponding reference commands for the system actuators, that are then rotated through serial communication. The reference orientation is continuously verified to make sure that solar tracker mobile platform does not perform unexpected motions.

V. EXPERIMENTAL RESULTS

In order to verify the develop system two test series were performed with the experimental setup described in Section IV-A. In the first test series the accuracy of the solar sensor is verified against the Sun Pointing Algorithm (SPA) [15]. The second test series analyses the pointing accuracy of the SPM platform.

A. Solar Sensor Accuracy Verification

For experimental studies the solar sensor was attached to the SPMs base, with the platform resting on a horizontal plane and MASS-60 x-axis aligned with magnetic-north vector. The Sun azimuth and elevation were recorded for some time intervals in both clear and cloudy conditions. Resulting angles were then compared with ones generated by the SPA. As illustrated in Fig. 10 there is a close correspondence between the solar sensor measurements and the SPA calculations. The RMS of an angle between vectors built with given elevation and azimuth across series is 6.3 degrees. Note that in the case when the Sun is obstructed by clouds, angles are interpolated and the overall result is smoothed. Ideally, when the Sun is obstructed the system will use the SPA for orientation determination.

The observed minor differences are attributed to the two main sources of errors. The first source of errors is the distortion of magnetic field in the work environment which adds a bias to the magnetic north vector. As a result, the transformation from the SPM coordinate system to a global coordinate system should be also filtered for bias. At current stage, the bias compensation is done manually, but the authors are going to implement a bias tracking routine in the final version of the algorithm. The second source of errors stems from assumptions and approximations made in the SPA. The SPA requires a large amount of inputs in order to calculate the Sun ephemeris precisely. Although currently the SPA operates with correct location and time, there are variables, i.e. pressure, temperature, density, etc., that are set to default values. In addition, one needs to keep in mind that in Kazakhstan GMT zones are rather large, so the precision of the local Sun time will be lacking slightly. In overall, the test series prove that the developed system is capable of locating the Sun regardless of weather conditions.

B. SPM Orientation Testing

For experimental validation of the platform orientation routine outlined in Section III, the SPM top mobile platform prototype was additionally equipped with an UM7-LT orientation sensor from CHRobotics [16] (Fig.11). This sensor combines triaxial accelerometer, rate gyro, and magnetometer data using a sophisticated extended Kalman filter to produce orientation estimates in the form of orientation quaternions. The sensor is attached to the SPM top platform in the way that it's local coordinate system is coincident with the SPM's one. In this way, the sensor directly measures the SPM's platform orientation. The experiential tests were performed using an Orient Sol3A solar simulator [17] (shown in Fig. 5) that facilitated high range motions of the solar tracker platform aiming at future work on mobile applications.

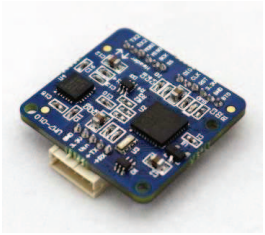

Fig. 11. UM7-LT orientation sensor [16]

.

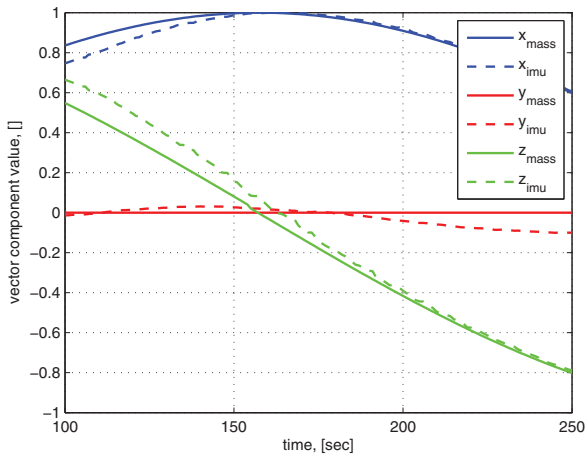

Fig. 12. Comparison of the x, y and z components of the SPM platform unit normal vector after rotation using a solar sensor based (MASS) and a orientation sensor (IMU) quaternions.

For this experiment the SPM platform was moved under the solar simulator. The quaternion processed from the solar angles was then used to rotate the SPM platform. Finally, the orientation quaternions generated by the IMU are compared with ones given by the solar sensor. Figure 12 presents the comparison of the x, y and z components of the unit normal vector after rotation using the solar sensor (MASS) measurement based quaternion and the UM7-LT sensor (IMU) quaternions showing actual state of the SPM prototype. The average RMS error for each axis components of the SPM unit normal vector is 4.87 degrees which is mostly attributed to the non-perfect mechanical state of the 3D-printed SPM prototype.

Based on the comparison results, it can be concluded that the proposed approach for the the SPM platform orientation estimation using the solar sensor measurements is correct and the 3-axis solar tracker platform can accurately orient itself towards the Sun.

VI. FUTURE WORK

The main advantage of the proposed 3-axis solar tracker platform over traditional 2-axis platforms is its applicability for designing mobile solar tracking platforms. There is a growing interest to design novel electric/hybrid vehicle based solar systems that can accumulate energy during time when the vehicle are parked on an open air. Adding solar tracking functionality into the vehicle solar systems regardless on the vehicle position and location (flat terrain, hills, slopes, etc.) will increase power generation efficiency. The authors are currently developing the platform inertial stabilization control to address this issue. The accompanying video of the SPM prototype inertial stabilization motion is available at www.alaris.kz. Further it is planned to improve tracking accuracy by fusing solar sensor data, SPA data, platform orientation, and accompanying biases through an Unscented Kalman filter to improve overall accuracy of the system.

REFERENCES

[1] H. Taghirad, *Parallel robots: mechanics and control*. CRC Press, 2013.

[2] C. Gosselin, E. St-Pierre, and M. Gagni, "On the development of the Agile Eye," *IEEE Robot. Automat. Mag.*, vol. 3, no. 4, pp. 29–37, 1996.

[3] F. Bidault, C. P. Teng, and J. Angeles, "Structural optimization of a spherical parallel manipulator using a two-level approach," in *Proc. ASME Design Engineering Tech. Conf.*, 2001.

[4] S. Bai, M. Hansen, and J. Angeles, "A robust forward-displacement analysis of spherical parallel robots," *Mech. Mach. Theory*, vol. 44, no. 12, pp. 2204–2216, 2009.

[5] Y.-K. Chang, B.-H. Lee, and S.-J. Kang, "High-accuracy image centroiding algorithm for cmos-based digital sun sensors," in *Sensors, 2007 IEEE*, Oct 2007, pp. 329–336.

[6] C. de Boom, J. Leijtens, L. v.Duivenbode, and N. van der Heiden, "Micro digital sun sensor: System in a package," in *MEMS, NANO and Smart Systems, 2004. ICMENS 2004. Proceedings. 2004 International Conference on*, Aug 2004, pp. 322–328.

[7] N. Xie and A. Theuwissen, "A miniaturized micro-digital sun sensor by means of low-power low-noise cmos imager," *Sensors Journal, IEEE*, vol. 14, no. 1, pp. 96–103, Jan 2014.

[8] "Solar-MEMS Sun Sensors," Website. [Online]. Available: http://www.solar-mems.com/en/products/space

[9] A. Niyetkaliyev and A. Shintemirov, "An approach for obtaining unique kinematic solutions of a spherical parallel manipulator," in *Proc. IEEE/ASME Int. Conf. Adv. Int. Mechatronics*, 2014, pp. 1355–1360.

[10] C. Gosselin, J. Sefrioui, and M. J. Richard, "On the direct kinematics of spherical three-degree-of-freedom parallel manipulators of general architecture," *ASME J. Mech. Des.*, vol. 116, no. 2, pp. 594–598, 1994.

[11] C. Gosselin and E. Lavoie, "On the kinematic design of spherical three-degree-of-freedom parallel manipulators," *Int. J. Robot. Res.*, vol. 12, no. 4, pp. 394–402, 1993.

[12] A. Shintemirov, A. Nyetkaliyev, and M. Rubagotti, "Numerical optimal control of a spherical parallel manipulator based on unique kinematic solutions," *IEEE/ASME Transactions on Mechatronics*, vol. in press, 2015.

[13] J. B. Kuipers, *Quaternions and Rotation Sequences: A Primer with Applications to Orbits, Aerospace and Virtual Reality*. Princeton University Press, 2002.

[14] "Qt Programming Environment," Website. [Online]. Available: http://www.qt.io

[15] I. Reda and A. Andreas, "Solar position algorithm for solar radiation applications," *Solar Energy*, vol. 76, no. 5, pp. 577–589, 2004.

[16] "UM7-LT Orientation Sensor," Website. [Online]. Available: http://www.chrobotics.com/shop/um7-lt-orientation-sensor

[17] "Oriel Sol3A Class AAA Solar Simulators," Website. [Online]. Available: http://www.newport.com/Class-AAA-Solar-Simulators/842468/1033/info.aspx